Inflationary three-point functions

L. Sriramkumar

Department of Physics, Indian Institute of Technology Madras, Chennai, India

The Primordial Universe After Planck

Institut d'Astrophysique de Paris, Paris

December 15–19, 2014

Plan of the talk

1. The status of inflationary models: Constraints from Planck
2. Some remarks on the computation of the power spectra during inflation
3. The Maldacena formalism for evaluating the scalar bispectrum
4. BINGO: An efficient code to numerically compute the bispectrum
5. Contributions to the scalar bispectrum during preheating
6. Evaluating the other three-point functions
7. The squeezed limit and the consistency relations
8. Summary

Conventions and notations

- Units: $c = \hbar = 1$, $M_{_{\rm Pl}} = (8\,\pi\,G)^{-1/2}$
- Background: Spatially flat FLRW metric described by the line-element
$$\mathrm{d}s^2 = -\mathrm{d}t^2 + a^2(t)\,\mathrm{d}\boldsymbol{x}^2 = a^2(\eta)\,\left(-\mathrm{d}\eta^2 + \mathrm{d}\boldsymbol{x}^2\right)$$
with t – cosmic time and η – conformal time
- Scale factor and Hubble parameter: a and $H = \dot{a}/a$
- Derivatives: $^{\cdot} \equiv \mathrm{d}/\mathrm{d}t$, $' \equiv \mathrm{d}/\mathrm{d}\eta$
- E-folds: N
- Curvature perturbation and its Fourier mode: $\mathcal{R}$ and $\mathcal{R}_{\boldsymbol{k}}$
- Tensor perturbation and its Fourier mode: γ_{ij} and $\gamma_{ij}^{\boldsymbol{k}}$

The latter part of this talk is based on. . .

- J. Martin and L. Sriramkumar, *The scalar bispectrum in the Starobinsky model: The equilateral case*, JCAP **1201**, 008 (2012).
- D. K. Hazra, J. Martin and L. Sriramkumar, *Scalar bispectrum during preheating in single field inflationary models*, Phys. Rev. D **86**, 063523 (2012).
- D. K. Hazra, L. Sriramkumar and J. Martin, *BINGO: A code for the efficient computation of the scalar bispectrum*, JCAP **1305**, 026 (2013).
- V. Sreenath, R. Tibrewala and L. Sriramkumar, *Numerical evaluation of the three-point scalar-tensor cross-correlations and the tensor bispectrum*, JCAP **1312**, 037 (2013).
- J. Martin, L. Sriramkumar and D. K. Hazra, *Sharp inflaton potentials and bi-spectra: Effects of smoothening the discontinuity*, JCAP **1409**, 039 (2014).
- V. Sreenath and L. Sriramkumar, *Examining the consistency relations describing the three-point functions involving tensors*, JCAP 1410, 021 (2014).
- V. Sreenath, D. K. Hazra and L. Sriramkumar, *On the scalar consistency relation away from slow roll*, arXiv:1410.0252 [astro-ph.CO].

The scalar and tensor power spectra

The scalar and tensor power spectra $\mathcal{P}_{_{\rm S}}(k)$ and $\mathcal{P}_{_{\rm T}}(k)$ are defined as:

$$\langle \hat{\mathcal{R}}_{\boldsymbol{k}}(\eta_{\rm e})\, \hat{\mathcal{R}}_{\boldsymbol{k}'}(\eta_{\rm e})\rangle = \frac{(2\,\pi)^2}{2\,k^3}\, \mathcal{P}_{_{\rm S}}(k)\; \delta^{(3)}\left(\boldsymbol{k}+\boldsymbol{k}'\right),$$

$$\langle \hat{\gamma}^{\boldsymbol{k}}_{m_1 n_1}(\eta_{\rm e})\, \hat{\gamma}^{\boldsymbol{k}'}_{m_2 n_2}(\eta_{\rm e})\rangle = \frac{(2\,\pi)^2}{8\,k^3}\, \Pi^{\boldsymbol{k}}_{m_1 n_1, m_2 n_2}\, \mathcal{P}_{_{\rm T}}(k)\; \delta^{3}\left(\boldsymbol{k}+\boldsymbol{k}'\right),$$

where $\eta_{\rm e}$ – conformal time towards the end of inflation and

$$\Pi^{\boldsymbol{k}}_{m_1 n_1, m_2 n_2} = \sum_{s} \varepsilon^{s}_{m_1 n_1}(\boldsymbol{k})\; \varepsilon^{s*}_{m_2 n_2}(\boldsymbol{k})$$

with $\varepsilon^{s}_{mn}(\boldsymbol{k})$ – polarization tensor describing the gravitational waves.

When comparing with the observations, one often uses the following power law, template scalar and tensor spectra:

$$\mathcal{P}_{_{\rm S}}(k) = \mathcal{A}_{_{\rm S}}\, \left(\frac{k}{k_\ast}\right)^{n_{_{\rm S}}-1} \quad \text{and} \quad \mathcal{P}_{_{\rm T}}(k) = \mathcal{A}_{_{\rm T}}\, \left(\frac{k}{k_\ast}\right)^{n_{_{\rm T}}}.$$

Constraints from cosmological data

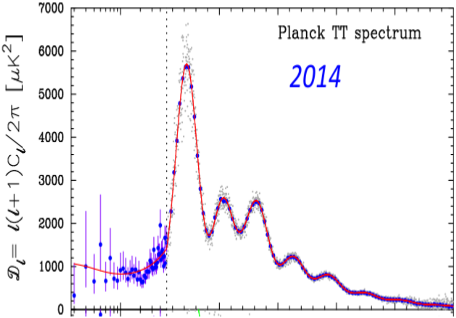

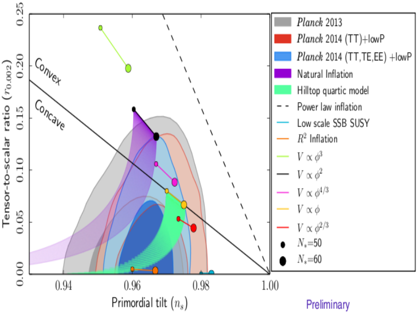

Left: The CMB TT angular power spectrum from the Planck 2014 data (the blue dots with error bars) and the theoretical, best fit ΛCDM model with a power law primordial spectrum (the solid red curve)[1].

Right: Joint constraints from the recent Planck data (and other cosmological data) on the inflationary parameters $n_{\rm S}$ and $r = \mathcal{P}_{\rm T}(k)/\mathcal{P}_{\rm S}(k)$[2].

1 From http://www.cosmos.esa.int/documents/387566/387653/Ferrara_Dec1_16h30_Efstathiou_Cosmology.pdf.

2 From http://www.cosmos.esa.int/documents/387566/387653/Ferrara_Dec3_14h30_Finelli_InflationPlanck.pdf.

Performance of inflationary models

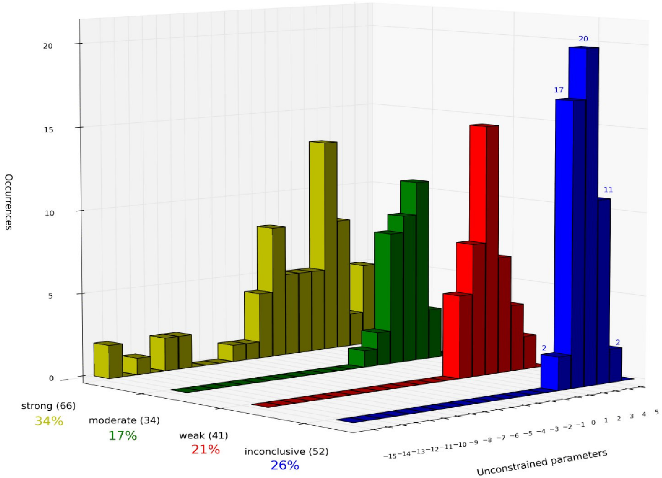

The efficiency of the inflationary paradigm leads to a situation wherein, despite the strong constraints, a variety of models continue to remain consistent with the data[3].

[3] J. Martin, C. Ringeval, R. Trotta and V. Vennin, JCAP **1403**, 039 (2014).

The scalar bispectrum

The scalar bispectrum $\mathcal{B}_{\mathcal{R}\mathcal{R}\mathcal{R}}(\boldsymbol{k}_1, \boldsymbol{k}_2, \boldsymbol{k}_3)$ evaluated towards the end of inflation at the conformal time η_{e} is defined as follows[4]:

$$\langle \hat{\mathcal{R}}_{\boldsymbol{k}_1}(\eta_{\mathrm{e}})\, \hat{\mathcal{R}}_{\boldsymbol{k}_2}(\eta_{\mathrm{e}})\, \hat{\mathcal{R}}_{\boldsymbol{k}_3}(\eta_{\mathrm{e}}) \rangle = (2\,\pi)^3\; \mathcal{B}_{\mathcal{R}\mathcal{R}\mathcal{R}}(\boldsymbol{k}_1, \boldsymbol{k}_2, \boldsymbol{k}_3)\; \delta^{(3)}\left(\boldsymbol{k}_1 + \boldsymbol{k}_2 + \boldsymbol{k}_3\right).$$

For convenience, we shall set

$$\mathcal{B}_{\mathcal{R}\mathcal{R}\mathcal{R}}(\boldsymbol{k}_1, \boldsymbol{k}_2, \boldsymbol{k}_3) = (2\,\pi)^{-9/2}\; G_{\mathcal{R}\mathcal{R}\mathcal{R}}(\boldsymbol{k}_1, \boldsymbol{k}_2, \boldsymbol{k}_3).$$

[4] D. Larson *et al.*, Astrophys. J. Suppl. **192**, 16 (2011);
E. Komatsu *et al.*, Astrophys. J. Suppl. **192**, 18 (2011).

The non-Gaussianity parameter $f_{\rm NL}$

The observationally relevant non-Gaussianity parameter $f_{\rm NL}$ is basically introduced through the relation[5]

$$\mathcal{R}(\eta, \boldsymbol{x}) = \mathcal{R}_{\rm G}(\eta, \boldsymbol{x}) - \frac{3\, f_{\rm NL}}{5}\, \left[\mathcal{R}_{\rm G}^2(\eta, \boldsymbol{x}) - \langle \mathcal{R}_{\rm G}^2(\eta, \boldsymbol{x})\rangle\right],$$

where $\mathcal{R}_{\rm G}$ denotes the Gaussian quantity.

Utilizing the above relation and Wick's theorem, one can arrive at

$$\begin{aligned}\langle \hat{\mathcal{R}}_{\boldsymbol{k}_1}\, \hat{\mathcal{R}}_{\boldsymbol{k}_2}\, \hat{\mathcal{R}}_{\boldsymbol{k}_3}\rangle &= -\frac{3\, f_{\rm NL}}{10}\, \frac{(2\,\pi)^{5/2}}{k_1^3\, k_2^3\, k_3^3}\, \delta^{(3)}(\boldsymbol{k}_1 + \boldsymbol{k}_2 + \boldsymbol{k}_3)\\ &\quad \times \left[k_1^3\, \mathcal{P}_{\rm S}(k_2)\, \mathcal{P}_{\rm S}(k_3) + \text{two permutations}\right],\end{aligned}$$

so that one obtains[6]

$$\begin{aligned}f_{\rm NL}(\boldsymbol{k}_1, \boldsymbol{k}_2, \boldsymbol{k}_3) &= -\frac{10}{3}\, \frac{1}{(2\,\pi)^4}\, \left(k_1^3\, k_2^3\, k_3^3\right)\, G_{\mathcal{R}\mathcal{R}\mathcal{R}}(\boldsymbol{k}_1, \boldsymbol{k}_2, \boldsymbol{k}_3)\\ &\quad \times \left[k_1^3\, \mathcal{P}_{\rm S}(k_2)\, \mathcal{P}_{\rm S}(k_3) + \text{two permutations}\right]^{-1}.\end{aligned}$$

[5] E. Komatsu and D. N. Spergel, Phys. Rev. D **63**, 063002 (2001).

[6] See, for example, J. Martin and L. Sriramkumar, JCAP **1201**, 008 (2012).

An illustration of the inflationary bispectrum

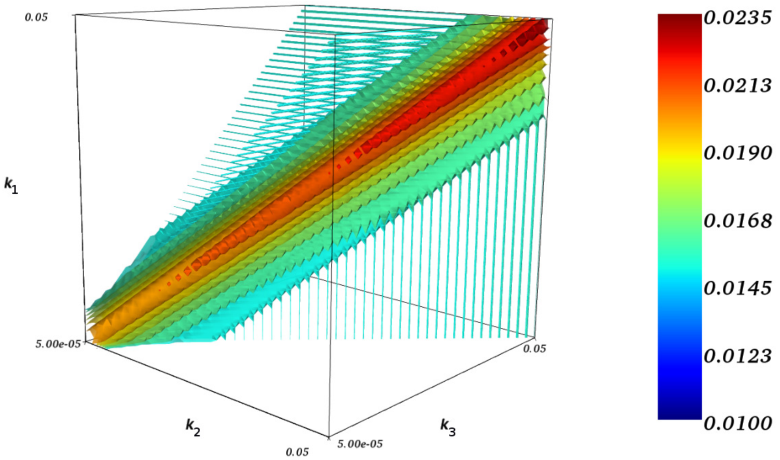

A typical scalar bispectrum encountered in slow roll inflation.

The observed CMB TTT angular bispectrum

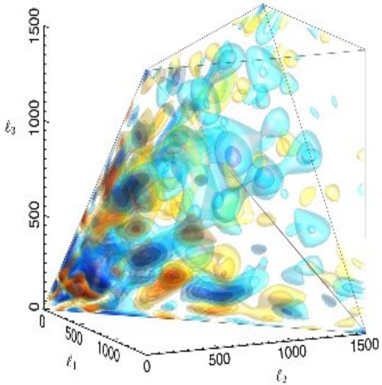

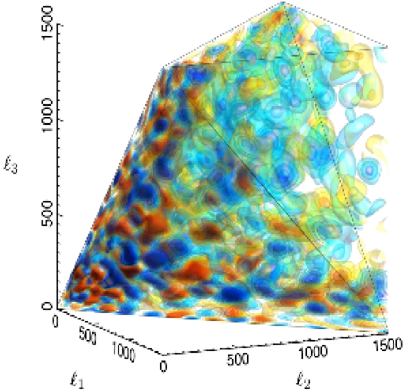

Left: The CMB TTT angular bispectrum as observed by Planck, in 2013[7].
Right: The corresponding 2014 result[8].

[7] P. A. R. Ade *et al.*, arXiv:1303.5084 [astro-ph.CO].

[8] From http://www.cosmos.esa.int/documents/387566/387653/Ferrara_Dec1_15h00_Wandelt_NG.pdf.

Template bispectra

For comparison with the observations, the scalar bispectrum is often expressed in terms of the parameters $f_{\rm NL}^{\rm loc}$, $f_{\rm NL}^{\rm eq}$ and $f_{\rm NL}^{\rm orth}$ as follows:

$$G_{\mathcal{RRR}}(\boldsymbol{k}_1, \boldsymbol{k}_2, \boldsymbol{k}_3) = f_{\rm NL}^{\rm loc}\, G_{\mathcal{RRR}}^{\rm loc}(\boldsymbol{k}_1, \boldsymbol{k}_2, \boldsymbol{k}_3) + f_{\rm NL}^{\rm eq}\, G_{\mathcal{RRR}}^{\rm eq}(\boldsymbol{k}_1, \boldsymbol{k}_2, \boldsymbol{k}_3) + f_{\rm NL}^{\rm orth}\, G_{\mathcal{RRR}}^{\rm orth}(\boldsymbol{k}_1, \boldsymbol{k}_2, \boldsymbol{k}_3).$$

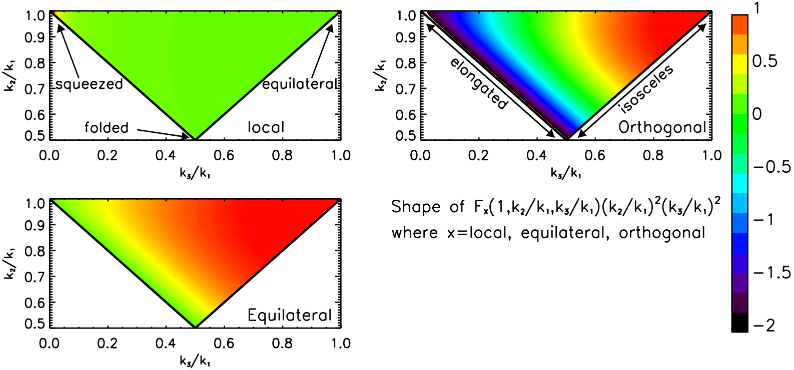

Illustration of the three template basis bispectra[9].

[9] E. Komatsu, Class. Quantum Grav. **27**, 124010 (2010).

Constraints on $f_{_{\rm NL}}$

The constraints on the primordial values of the non-Gaussianity parameters from the Planck data are as follows[10]:

2013 results

$$\begin{aligned} f_{_{\rm NL}}^{\rm loc} &= 2.7 \pm 5.8, \\ f_{_{\rm NL}}^{\rm eq} &= -42 \pm 75, \\ f_{_{\rm NL}}^{\rm orth} &= -25 \pm 39. \end{aligned}$$

2014 results

$$\begin{aligned} f_{_{\rm NL}}^{\rm loc} &= 0.71 \pm 5.1, \\ f_{_{\rm NL}}^{\rm eq} &= -9.5 \pm 44, \\ f_{_{\rm NL}}^{\rm orth} &= -25 \pm 22. \end{aligned}$$

Note that the constraints on each of the $f_{_{\rm NL}}$ parameters have been arrived at assuming that the other two parameters are zero.

We should also add that these constraints become less stringent if the primordial spectra are assumed to contain features.

These constraints imply that slowly rolling single field models involving the canonical scalar field which are favored by the data at the level of power spectra are also consistent with the data at the level of non-Gaussianities.

[10] P. A. R. Ade *et al.*, Astron. Astrophys. **571**, A24 (2014);

From http://www.cosmos.esa.int/documents/387566/387653/Ferrara_Dec3_14h50_Bartolo_PSandBispectrum.pdf.

Quantization and power spectra

On quantization, the operators $\hat{\mathcal{R}}(\eta, \boldsymbol{x})$ and $\hat{\gamma}_{ij}(\eta, \boldsymbol{x})$ can be expressed as[11]

$$\hat{\mathcal{R}}(\eta, \boldsymbol{x}) = \int \frac{\mathrm{d}^3\boldsymbol{k}}{(2\,\pi)^{3/2}} \left[\hat{a}_{\boldsymbol{k}}\, f_k(\eta)\, \mathrm{e}^{i\,\boldsymbol{k}\cdot\boldsymbol{x}} + \hat{a}^{\dagger}_{\boldsymbol{k}}\, f^{*}_k(\eta)\, \mathrm{e}^{-i\,\boldsymbol{k}\cdot\boldsymbol{x}}\right],$$

$$\hat{\gamma}_{ij}(\eta, \boldsymbol{x}) = \sum_s \int \frac{\mathrm{d}^3\boldsymbol{k}}{(2\,\pi)^{3/2}} \left[\hat{b}^{s}_{\boldsymbol{k}}\, \varepsilon^{s}_{ij}(\boldsymbol{k})\, g_k(\eta)\, \mathrm{e}^{i\,\boldsymbol{k}\cdot\boldsymbol{x}} + \hat{b}^{s\dagger}_{\boldsymbol{k}}\, \varepsilon^{s*}_{ij}(\boldsymbol{k})\, g^{*}_k(\eta)\, \mathrm{e}^{-i\,\boldsymbol{k}\cdot\boldsymbol{x}}\right],$$

where the Fourier modes f_k and g_k satisfy the following equations of motion:

$$f_k'' + 2\,(z'/z)\, f_k' + k^2\, f_k = 0 \quad \text{and} \quad g_k'' + 2\,(a'/a)\, g_k' + k^2\, g_k = 0,$$

with $z = a\, M_{_{\mathrm{Pl}}}\, \sqrt{2\,\epsilon_1}$ and $\epsilon_1 = -\,\mathrm{d} \ln H/\mathrm{d}N$ being the first slow roll parameter.

In the vacuum state annihilated by the operators $\hat{a}_{\boldsymbol{k}}$ and $\hat{b}^{s}_{\boldsymbol{k}}$, the power spectra are given by the expressions

$$\mathcal{P}_{_{\mathrm{S}}}(k) = \frac{k^3}{2\,\pi^2}\, |f_k|^2 \quad \text{and} \quad \mathcal{P}_{_{\mathrm{T}}}(k) = 4\, \frac{k^3}{2\,\pi^2}\, |g_k|^2.$$

With the initial conditions imposed in the sub-Hubble domain, *viz.* when $k/(a\,H) \gg 1$, these spectra are to be evaluated on super-Hubble scales, *i.e.* as $k/(a\,H) \ll 1$.

[11] See, for instance, L. Sriramkumar, Curr. Sci. **97**, 868 (2009).

From inside the Hubble radius to super-Hubble scales

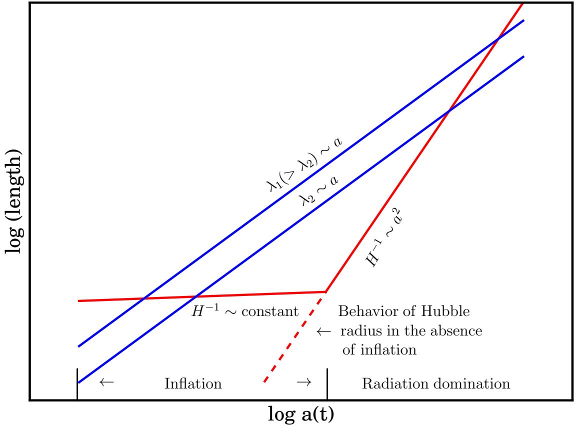

A schematic diagram illustrating the behavior of the physical wavelength $\lambda_{\rm P} \propto a$ (the blue lines) and the Hubble radius H^{-1} (the red line) during inflation and the radiation dominated epochs[12].

[12] See, for example, E. W. Kolb and M. S. Turner, *The Early Universe* (Addison-Wesley Publishing Company, New York, 1990), Fig. 8.4.

The quadratic action governing the perturbations

The actions governing the perturbations at a given order can be arrived at using the ADM formalism.

For instance, one can work in a gauge wherein, upon taking into account the scalar and the tensor perturbations, the FLRW metric is described by the line-element

$$\mathrm{d}s^2 = -\mathrm{d}t^2 + a^2(t)\, \mathrm{e}^{2\,\mathcal{R}(t,\boldsymbol{x})}\, \left[\mathrm{e}^{\gamma(t,\boldsymbol{x})}\right]_{ij} \mathrm{d}\boldsymbol{x}^i \mathrm{d}\boldsymbol{x}^j.$$

One can show that, at the quadratic order, the actions governing $\mathcal{R}$ and γ_{ij} are given by[13]

$$\mathcal{S}^2_{\mathcal{R}\mathcal{R}}[\mathcal{R}] = \frac{1}{2} \int \mathrm{d}\eta \int \mathrm{d}^3\boldsymbol{x}\;\, z^2\, \left[\mathcal{R}'^2 - (\partial\mathcal{R})^2\right],$$

and

$$\mathcal{S}^2_{\gamma\gamma}[\gamma_{ij}] = \frac{M_{_{\mathrm{Pl}}}^2}{8} \int \mathrm{d}\eta \int \mathrm{d}^3\boldsymbol{x}\;\, a^2\, \left[\gamma_{ij}'^{\,2} - (\partial\gamma_{ij})^2\right].$$

[13] V. F. Mukhanov, H. A. Feldman and R. H. Brandenberger, Phys. Rep. **215**, 203 (1992).

The action at the cubic order

It can be shown that the third order term in the action describing the curvature perturbation is given by[14]

$$\begin{aligned}\mathcal{S}^3_{\mathcal{R}\mathcal{R}\mathcal{R}}[\mathcal{R}] = M_{_{\rm Pl}}^2 \int {\rm d}\eta \int {\rm d}^3\boldsymbol{x}\, \biggl[& a^2\, \epsilon_1^2\, \mathcal{R}\, \mathcal{R}'^2 + a^2\, \epsilon_1^2\, \mathcal{R}\, (\partial\mathcal{R})^2 \\ & - 2\, a\, \epsilon_1\, \mathcal{R}'\, (\partial^i\mathcal{R})\, (\partial_i\chi) + \frac{a^2}{2}\, \epsilon_1\, \epsilon_2'\, \mathcal{R}^2\, \mathcal{R}' + \frac{\epsilon_1}{2}\, (\partial^i\mathcal{R})\, (\partial_i\chi)\, (\partial^2\chi) \\ & + \frac{\epsilon_1}{4}\, (\partial^2\mathcal{R})\, (\partial\chi)^2 + \mathcal{F}^1(\mathcal{R})\, \frac{\delta\mathcal{L}^2_{\mathcal{R}\mathcal{R}}}{\delta\mathcal{R}}\biggr],\end{aligned}$$

where $\epsilon_2 = {\rm d}\ln\epsilon_1/{\rm d}N$ is the second slow roll parameter, $\mathcal{L}^2_{\mathcal{R}\mathcal{R}}$ represents the second order Lagrangian density governing the scalars, and $\partial^2\chi = a\, \epsilon_1\, \mathcal{R}'$.

[14] J. Maldacena, JHEP **0305**, 013 (2003);
D. Seery and J. E. Lidsey, JCAP **0506**, 003 (2005);
X. Chen, M.-x. Huang, S. Kachru and G. Shiu, JCAP **0701**, 002 (2007).

Evaluating the scalar bispectrum

At the leading order in the perturbations, one then finds that the scalar three-point correlation function in Fourier space is described by the integral[15]

$$\langle\hat{\mathcal{R}}_{\boldsymbol{k}_1}(\eta_{\mathrm{e}})\,\hat{\mathcal{R}}_{\boldsymbol{k}_2}(\eta_{\mathrm{e}})\,\hat{\mathcal{R}}_{\boldsymbol{k}_3}(\eta_{\mathrm{e}})\rangle = -i\int_{\eta_{\mathrm{i}}}^{\eta_{\mathrm{e}}} \mathrm{d}\eta\; a(\eta)\;\left\langle\left[\hat{\mathcal{R}}_{\boldsymbol{k}_1}(\eta_{\mathrm{e}})\,\hat{\mathcal{R}}_{\boldsymbol{k}_2}(\eta_{\mathrm{e}})\,\hat{\mathcal{R}}_{\boldsymbol{k}_3}(\eta_{\mathrm{e}}),\hat{H}_{\mathrm{I}}(\eta)\right]\right\rangle,$$

where $\hat{H}_{\mathrm{I}}$ is the Hamiltonian corresponding to the above third order action and η_{i} denotes a sufficiently early time when the initial conditions are imposed on the modes.

Note that, while the square brackets imply the commutation of the operators, the angular brackets denote the fact that the correlations are to be evaluated in the perturbative vacuum.

[15] See, for example, D. Seery and J. E. Lidsey, JCAP **0506**, 003 (2005); X. Chen, Adv. Astron. **2010**, 638979 (2010).

The resulting bispectrum

The quantity $G_{\mathcal{RRR}}(\boldsymbol{k}_1, \boldsymbol{k}_2, \boldsymbol{k}_3)$ evaluated towards the end of inflation at the conformal time $\eta_{\rm e}$ can be written as[16]

$$\begin{aligned} G_{\mathcal{RRR}}(\boldsymbol{k}_1, \boldsymbol{k}_2, \boldsymbol{k}_3) &\equiv \sum_{C=1}^{7} G_{\mathcal{RRR}}^{(C)}(\boldsymbol{k}_1, \boldsymbol{k}_2, \boldsymbol{k}_3) \\ &\equiv M_{\rm Pl}^2 \sum_{C=1}^{6} \Big\{ \left[f_{k_1}(\eta_{\rm e})\, f_{k_2}(\eta_{\rm e})\, f_{k_3}(\eta_{\rm e})\right]\, \mathcal{G}_{\mathcal{RRR}}^{(C)}(\boldsymbol{k}_1, \boldsymbol{k}_2, \boldsymbol{k}_3) \\ &\qquad + \text{complex conjugate} \Big\} + G_{\mathcal{RRR}}^{(7)}(\boldsymbol{k}_1, \boldsymbol{k}_2, \boldsymbol{k}_3), \end{aligned}$$

where the quantities $\mathcal{G}_{\mathcal{RRR}}^{(C)}(\boldsymbol{k}_1, \boldsymbol{k}_2, \boldsymbol{k}_3)$ with $C = (1, 6)$ correspond to the six terms in the interaction Hamiltonian.

The additional, seventh term $G_{\mathcal{RRR}}^{(7)}(\boldsymbol{k}_1, \boldsymbol{k}_2, \boldsymbol{k}_3)$ arises due to a field redefinition, and its contribution to $G_{\mathcal{RRR}}(\boldsymbol{k}_1, \boldsymbol{k}_2, \boldsymbol{k}_3)$ is given by

$$G_{\mathcal{RRR}}^{(7)}(\boldsymbol{k}_1, \boldsymbol{k}_2, \boldsymbol{k}_3) = \frac{\epsilon_2(\eta_{\rm e})}{2}\, \left(\left|f_{k_2}(\eta_{\rm e})\right|^2 \left|f_{k_3}(\eta_{\rm e})\right|^2 + \text{two permutations}\right).$$

[16] J. Martin and L. Sriramkumar, JCAP **1201**, 008 (2012).

The integrals involved

The quantities $\mathcal{G}^{(C)}_{\mathcal{R}\mathcal{R}\mathcal{R}}(\boldsymbol{k}_1, \boldsymbol{k}_2, \boldsymbol{k}_3)$ with $C = (1, 6)$ are described by the integrals

$$\mathcal{G}^{(1)}_{\mathcal{R}\mathcal{R}\mathcal{R}}(\boldsymbol{k}_1, \boldsymbol{k}_2, \boldsymbol{k}_3) \;=\; 2\,i \int_{\eta_{\rm i}}^{\eta_{\rm e}} {\rm d}\eta\, a^2\, \epsilon_1^2\, \left(f_{k_1}^{\ast}\, f_{k_2}^{\prime\ast}\, f_{k_3}^{\prime\ast} + \text{two permutations}\right),$$

$$\mathcal{G}^{(2)}_{\mathcal{R}\mathcal{R}\mathcal{R}}(\boldsymbol{k}_1, \boldsymbol{k}_2, \boldsymbol{k}_3) \;=\; -\,2\,i\, \left(\boldsymbol{k}_1\cdot\boldsymbol{k}_2 + \text{two permutations}\right) \int_{\eta_{\rm i}}^{\eta_{\rm e}} {\rm d}\eta\, a^2\, \epsilon_1^2\, f_{k_1}^{\ast}\, f_{k_2}^{\ast}\, f_{k_3}^{\ast},$$

$$\mathcal{G}^{(3)}_{\mathcal{R}\mathcal{R}\mathcal{R}}(\boldsymbol{k}_1, \boldsymbol{k}_2, \boldsymbol{k}_3) \;=\; -\,2\,i \int_{\eta_{\rm i}}^{\eta_{\rm e}} {\rm d}\eta\, a^2\, \epsilon_1^2\, \left[\left(\frac{\boldsymbol{k}_1\cdot\boldsymbol{k}_2}{k_2^2}\right) f_{k_1}^{\ast}\, f_{k_2}^{\prime\ast}\, f_{k_3}^{\prime\ast} + \text{five permutations}\right],$$

$$\mathcal{G}^{(4)}_{\mathcal{R}\mathcal{R}\mathcal{R}}(\boldsymbol{k}_1, \boldsymbol{k}_2, \boldsymbol{k}_3) \;=\; i \int_{\eta_{\rm i}}^{\eta_{\rm e}} {\rm d}\eta\, a^2\, \epsilon_1\, \epsilon_2^{\prime}\, \left(f_{k_1}^{\ast}\, f_{k_2}^{\ast}\, f_{k_3}^{\prime\ast} + \text{two permutations}\right),$$

$$\mathcal{G}^{(5)}_{\mathcal{R}\mathcal{R}\mathcal{R}}(\boldsymbol{k}_1, \boldsymbol{k}_2, \boldsymbol{k}_3) \;=\; \frac{i}{2} \int_{\eta_{\rm i}}^{\eta_{\rm e}} {\rm d}\eta\, a^2\, \epsilon_1^3\, \left[\left(\frac{\boldsymbol{k}_1\cdot\boldsymbol{k}_2}{k_2^2}\right) f_{k_1}^{\ast}\, f_{k_2}^{\prime\ast}\, f_{k_3}^{\prime\ast} + \text{five permutations}\right],$$

$$\mathcal{G}^{(6)}_{\mathcal{R}\mathcal{R}\mathcal{R}}(\boldsymbol{k}_1, \boldsymbol{k}_2, \boldsymbol{k}_3) \;=\; \frac{i}{2} \int_{\eta_{\rm i}}^{\eta_{\rm e}} {\rm d}\eta\, a^2\, \epsilon_1^3\, \left\{\left[\frac{k_1^2\, (\boldsymbol{k}_2\cdot\boldsymbol{k}_3)}{k_2^2\, k_3^2}\right] f_{k_1}^{\ast}\, f_{k_2}^{\prime\ast}\, f_{k_3}^{\prime\ast} + \text{two permutations}\right\}.$$

The analytical scalar bispectrum in slow roll inflation

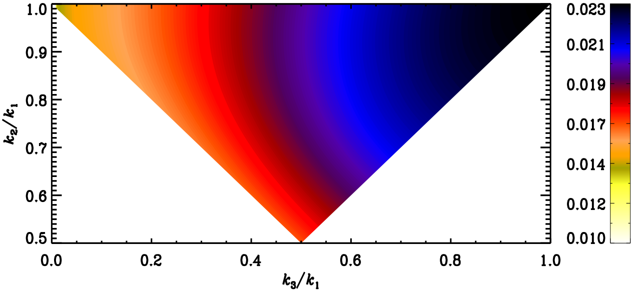

The inflationary scalar bispectrum (actually, the non-Gaussianity parameter $f_{\rm NL}$) in the case of the conventional quadratic potential, arrived at analytically using the slow roll approximation[17].

Note that $f_{\rm NL} \sim \epsilon_1$ in canonical models involving a single scalar field, while $f_{\rm NL} \sim \epsilon_1/c_{\rm S}^2$ in non-canonical models, where $c_{\rm S}$ denotes the speed of the scalar perturbations[18]. The most recent results imply that $c_{\rm S} \geq 0.024$[19].

[17] D. K. Hazra, L. Sriramkumar and J. Martin, JCAP **1305**, 026 (2013).

[18] See, for example, D. Seery and J. E. Lidsey, JCAP **0506**, 003 (2005); X. Chen, Adv. Astron. **2010**, 638979 (2010).

[19] From http://www.cosmos.esa.int/documents/387566/387653/Ferrara_Dec3_14h50_Bartolo_PSandBispectrum.pdf.

The various times of interest[20]

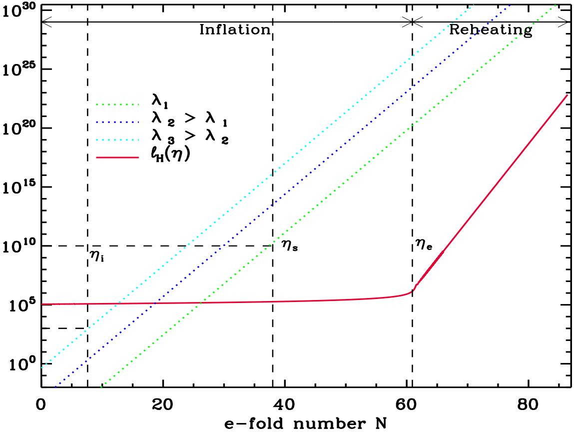

The exact behavior of the physical wavelengths and the Hubble radius plotted as a function of the number of e-folds in the case of the archetypical quadratic potential, which allows us to illustrate the various times of our interest, *viz.* η_{i}, η_{s} and η_{e}.

[20] D. K. Hazra, L. Sriramkumar and J. Martin, JCAP **1305**, 026 (2013).

An estimate of the super-Hubble contribution to $f_{\rm NL}^{\rm eq}$

In power law inflation of the form $a(\eta) = a_1\,(\eta/\eta_1)^{\gamma+1}$, one can show that the super-Hubble contribution to $f_{_{\rm NL}}$ in the equilateral limit is given by

$$f_{_{\rm NL}}^{{\rm eq}\,({\rm se})}(k) = \frac{5}{72\,\pi}\,\left[12 - \frac{9\,(\gamma+2)}{\gamma+1}\right]\,\Gamma^2\left(\gamma+\frac{1}{2}\right)\,2^{2\,\gamma+1}\,(2\,\gamma+1)\,(\gamma+2)$$

$$\times\,(\gamma+1)^{-2\,(\gamma+1)}\,\sin\left(2\,\pi\,\gamma\right)\,\left[1-\frac{H_{\rm s}}{H_{\rm e}}\,{\rm e}^{-3\,(N_{\rm e}-N_{\rm s})}\right]\,\left(\frac{k}{a_{\rm s}\,H_{\rm s}}\right)^{-(2\,\gamma+1)},$$

where we have set η_1 to be η_s.

For $\gamma = -(2+\varepsilon)$, where $\varepsilon \simeq 10^{-2}$, the above estimate for $f_{_{\rm NL}}$ reduces to

$$f_{_{\rm NL}}^{{\rm eq}\,({\rm se})}(k) \lesssim -\frac{5\,\varepsilon^2}{9}\,\left(\frac{k_{\rm s}}{a_{\rm s}\,H_{\rm s}}\right)^3 \simeq -10^{-19},$$

where, in obtaining the final value, we have set $k_{\rm s}/(a_{\rm s}\,H_{\rm s}) = 10^{-5}$.

Implementation of the cut-off in the sub-Hubble limit

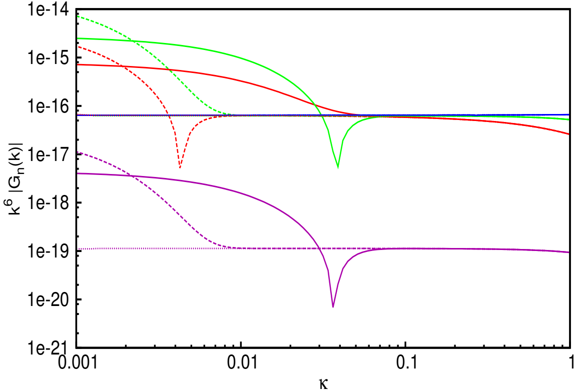

The various contributions to the bispectrum, with the sub-Hubble cut-off introduced as $\exp - \kappa\, k/(a\, H)$, have been plotted as a function of the parameter κ for a given mode and a fixed upper limit in the case of the quadratic inflationary potential[21]. The solid, dashed and the dotted lines correspond to integrating from $k/(a\, H)$ of 10^2, 10^3 and 10^4, respectively. Clearly, $\kappa = 0.1$ seems to be an optimal value[22].

[21] X. Chen, R. Easther and E. A. Lim, JCAP **0706**, 023 (2007); JCAP **0804**, 010 (2008).

[22] D. K. Hazra, L. Sriramkumar and J. Martin, JCAP **1305**, 026, (2013).

Results from BINGO[23]

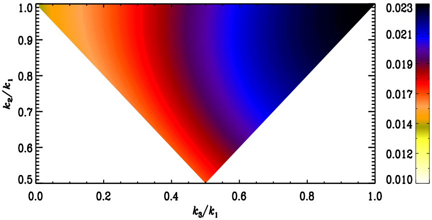

A comparison of the analytical results (on the left) for the non-Gaussianity parameter $f_{\rm NL}$ with the numerical results from the code BIspectra and Non-Gaussianity Operator or, simply, BINGO (on the right) for a generic triangular configuration of the wavevectors in the case of the standard quadratic potential. The maximum difference between the numerical and the analytic results is found to be about 5%.

[23] D. K. Hazra, L. Sriramkumar and J. Martin, JCAP **1305**, 026, (2013).

Inflationary models permitting deviations from slow roll

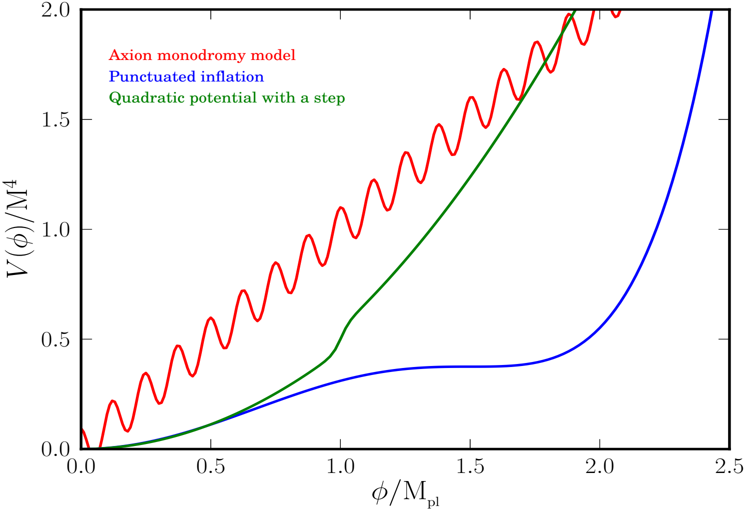

Illustration of potentials that admit departures from slow roll.

Spectra leading to an improved fit to the CMB data

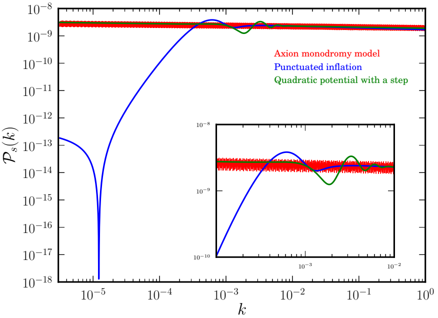

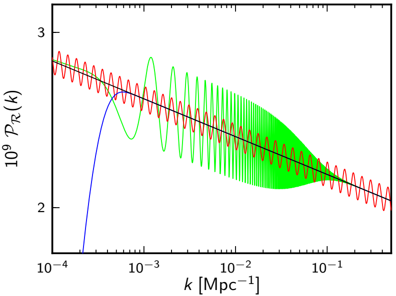

Left: The scalar power spectra in different inflationary models that lead to a better fit to the CMB data than the conventional power law spectrum[24].
Right: A set of spectra with features considered by the Planck team[25].

---

[24] R. K. Jain, P. Chingangbam, J.-O. Gong, L. Sriramkumar and T. Souradeep, JCAP **0901**, 009 (2009); D. K. Hazra, M. Aich, R. K. Jain, L. Sriramkumar and T. Souradeep, JCAP **1010**, 008 (2010); M. Aich, D. K. Hazra, L. Sriramkumar and T. Souradeep, Phys. Rev. D **87**, 083526 (2013).

[25] P. A. R. Ade *et al.*, Astron. Astrophys. **571**, A22 (2014).

$f_{\rm NL}$ in models with features[26]

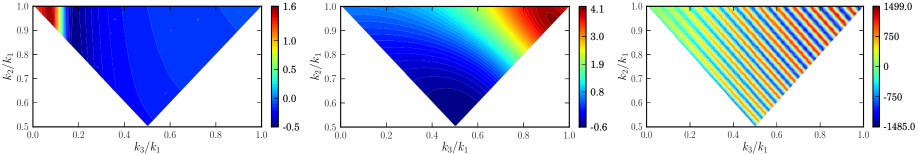

The scalar non-Gaussianity parameter $f_{\rm NL}$ in the punctuated inflationary scenario (on the left), quadratic potential with a step (in the middle) and the axion monodromy model (on the right).

[26] D. K. Hazra, L. Sriramkumar and J. Martin, JCAP **1305**, 026 (2013);
V. Sreenath, D. K. Hazra and L. Sriramkumar, arXiv:1410.0252 [astro-ph.CO].

Evolution during preheating

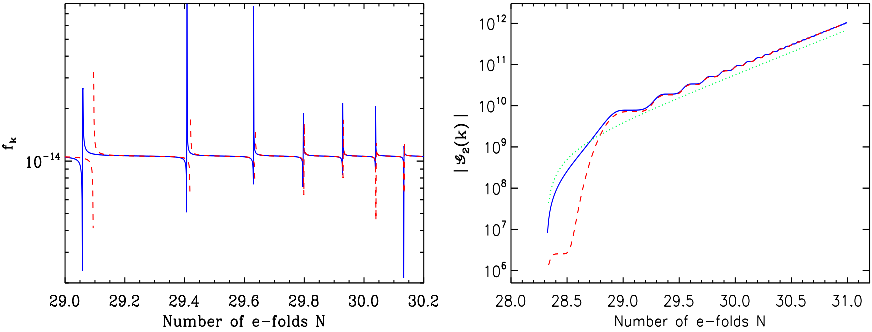

Left: The evolution of the curvature perturbation associated with a very small scale mode during preheating in a quadratic minimum.
Right: The behavior of the corresponding $\mathcal{G}_2(\boldsymbol{k}_1, \boldsymbol{k}_2, \boldsymbol{k}_3)$ in the equilateral limit. The blue curves represent the numerical results, while the dashed red curves denote the analytical results.

An estimate of the contribution to $f_{_{\rm NL}}^{\rm eq}$ during preheating

Upon assuming inflation to be of the power law form, the contribution to the non-Gaussianity parameter $f_{_{\rm NL}}$ during preheating can be obtained to be

$$\begin{aligned} f_{_{\rm NL}}^{\rm eq}(k) &= \frac{115\,\epsilon_1}{288\,\pi}\,\Gamma^2\left(\gamma+\frac{1}{2}\right)\,2^{2\,\gamma+1}\,\left(2\,\gamma+1\right)^2\,\sin\left(2\,\pi\,\gamma\right)\,\vert\gamma+1\vert^{-2\,(\gamma+1)} \\ &\quad\times\left[1-{\rm e}^{-3\,(N_{\rm f}-N_{\rm e})/2}\right]\,\left[\left(\frac{\pi^2\,g_\ast}{30}\right)^{-1/4}\,\left(1+z_{\rm eq}\right)^{1/4}\,\frac{\rho_{\rm cri}^{1/4}}{T_{\rm rh}}\right]^{-(2\,\gamma+1)} \\ &\quad\times\left(\frac{k}{a_0\,H_0}\right)^{-(2\,\gamma+1)}, \end{aligned}$$

where $g_\ast$ denotes the effective number of relativistic degrees of freedom at reheating, $T_{\rm rh}$ the reheating temperature and $z_{\rm eq}$ the redshift at the epoch of equality. Also, $\rho_{\rm cri}$, a_0 and H_0 represent the critical energy density, the scale factor and the Hubble parameter today, respectively.

For a model with $\gamma\simeq -2$ and a reheating temperature of $T_{\rm rh}\simeq 10^{10}$ GeV, one obtains that $f_{_{\rm NL}}\approx 10^{-60}$ for the modes of cosmological interest (*i.e.* for k such that $k/a_0\simeq H_0$), a value which is completely unobservable[27].

[27] D. K. Hazra, J. Martin and L. Sriramkumar, Phys. Rev. D **86**, 063523 (2012).

The cross-correlations and the tensor bispectrum

The cross-correlations involving two scalars and a tensor and a scalar and two tensors are defined as

$$\langle \hat{\mathcal{R}}_{\boldsymbol{k}_1}(\eta_{\rm e})\, \hat{\mathcal{R}}_{\boldsymbol{k}_2}(\eta_{\rm e})\, \hat{\gamma}^{\boldsymbol{k}_3}_{m_3 n_3}(\eta_{\rm e})\,\rangle = (2\,\pi)^3\, \mathcal{B}^{m_3 n_3}_{\mathcal{R}\mathcal{R}\gamma}(\boldsymbol{k}_1, \boldsymbol{k}_2, \boldsymbol{k}_3)\; \delta^{(3)}\,(\boldsymbol{k}_1 + \boldsymbol{k}_2 + \boldsymbol{k}_3)\,,$$

$$\langle \hat{\mathcal{R}}_{\boldsymbol{k}_1}(\eta_{\rm e})\, \hat{\gamma}^{\boldsymbol{k}_2}_{m_2 n_2}(\eta_{\rm e})\, \hat{\gamma}^{\boldsymbol{k}_3}_{m_3 n_3}(\eta_{\rm e})\rangle = (2\,\pi)^3\, \mathcal{B}^{m_2 n_2 m_3 n_3}_{\mathcal{R}\gamma\gamma}(\boldsymbol{k}_1, \boldsymbol{k}_2, \boldsymbol{k}_3) \times \delta^{(3)}\,(\boldsymbol{k}_1 + \boldsymbol{k}_2 + \boldsymbol{k}_3)\,,$$

while the tensor bispectrum is given by

$$\langle \hat{\gamma}^{\boldsymbol{k}_1}_{m_1 n_1}(\eta_{\rm e})\, \hat{\gamma}^{\boldsymbol{k}_2}_{m_2 n_2}(\eta_{\rm e})\, \hat{\gamma}^{\boldsymbol{k}_3}_{m_3 n_3}(\eta_{\rm e})\rangle = (2\,\pi)^3\, \mathcal{B}^{m_1 n_1 m_2 n_2 m_3 n_3}_{\gamma\gamma\gamma}(\boldsymbol{k}_1, \boldsymbol{k}_2, \boldsymbol{k}_3) \times \delta^{(3)}\,(\boldsymbol{k}_1 + \boldsymbol{k}_2 + \boldsymbol{k}_3)\,.$$

As in the pure scalar case, we shall set

$$\mathcal{B}_{\mathsf{ABC}}(\boldsymbol{k}_1, \boldsymbol{k}_2, \boldsymbol{k}_3) = (2\,\pi)^{-9/2}\; G_{\mathsf{ABC}}(\boldsymbol{k}_1, \boldsymbol{k}_2, \boldsymbol{k}_3),$$

where each of $(\mathsf{A}, \mathsf{B}, \mathsf{C})$ can be either a $\mathcal{R}$ or a γ.

Introducing additional non-Gaussianity parameters

Extending the original argument for introducing the parameter $f_{_{\rm NL}}$, one can introduce dimensionless non-Gaussianity parameters, say, $C_{_{\rm NL}}^{\mathcal{R}}$, $C_{_{\rm NL}}^{\gamma}$ and $h_{_{\rm NL}}$, to characterize the other three-point functions as follows[28]:

$$\begin{aligned}\mathcal{R}(\eta,\boldsymbol{x}) &= \mathcal{R}_{_{\rm G}}(\eta,\boldsymbol{x}) - \frac{3\,f_{_{\rm NL}}}{5}\,\left[\mathcal{R}_{_{\rm G}}^2(\eta,\boldsymbol{x}) - \langle\mathcal{R}_{_{\rm G}}^2(\eta,\boldsymbol{x})\rangle\right]\\ &\quad - C_{_{\rm NL}}^{\mathcal{R}}\,\mathcal{R}_{_{\rm G}}(\eta,\boldsymbol{x})\,\gamma_{\bar{m}\bar{n}}^{\rm G}(\eta,\boldsymbol{x})\end{aligned}$$

and

$$\begin{aligned}\gamma_{ij}(\eta,\boldsymbol{x}) &= \gamma_{ij}^{\rm G}(\eta,\boldsymbol{x}) - h_{_{\rm NL}}\,\left[\gamma_{ij}^{\rm G}(\eta,\boldsymbol{x})\,\gamma_{\bar{m}\bar{n}}^{\rm G}(\eta,\boldsymbol{x}) - \langle\gamma_{ij}^{\rm G}(\eta,\boldsymbol{x})\,\gamma_{\bar{m}\bar{n}}^{\rm G}(\eta,\boldsymbol{x})\rangle\right]\\ &\quad - C_{_{\rm NL}}^{\gamma}\,\gamma_{ij}^{\rm G}(\eta,\boldsymbol{x})\,\mathcal{R}_{_{\rm G}}(\eta,\boldsymbol{x}),\end{aligned}$$

where $\mathcal{R}_{_{\rm G}}$ and $\gamma_{ij}^{\rm G}$ denote the Gaussian quantities.

[28] V. Sreenath, R. Tibrewala and L. Sriramkumar, JCAP **1312**, 037 (2013).

Expressions for the non-Gaussianity parameters

One finds that the non-Gaussianity parameters $C_{\rm NL}^{\mathcal{R}}$, $C_{\rm NL}^{\gamma}$ and $h_{\rm NL}$ can be expressed in terms of the scalar-scalar-tensor and the scalar-tensor-tensor cross-correlations and the tensor bispectrum as[29]

$$
\begin{aligned}
C_{\rm NL}^{\mathcal{R}} &= -\frac{4}{(2\,\pi^2)^2}\,\left[k_1^3\,k_2^3\,k_3^3\,G_{\mathcal{R}\mathcal{R}\gamma}^{m_3 n_3}(\boldsymbol{k}_1,\boldsymbol{k}_2,\boldsymbol{k}_3)\right] \\
&\quad\times\left(\Pi_{m_3 n_3,\bar{m}\bar{n}}^{\boldsymbol{k}_3}\right)^{-1}\,\left\{\left[k_1^3\,\mathcal{P}_{_{\rm S}}(k_2)+k_2^3\,\mathcal{P}_{_{\rm S}}(k_1)\right]\,\mathcal{P}_{_{\rm T}}(k_3)\right\}^{-1}, \\
C_{\rm NL}^{\gamma} &= -\frac{4}{(2\,\pi^2)^2}\,\left[k_1^3\,k_2^3\,k_3^3\,G_{\mathcal{R}\gamma\gamma}^{m_2 n_2 m_3 n_3}(\boldsymbol{k}_1,\boldsymbol{k}_2,\boldsymbol{k}_3)\right] \\
&\quad\times\left\{\mathcal{P}_{_{\rm S}}(k_1)\,\left[\Pi_{m_2 n_2,m_3 n_3}^{\boldsymbol{k}_2}\,k_3^3\,\mathcal{P}_{_{\rm T}}(k_2)+\Pi_{m_3 n_3,m_2 n_2}^{\boldsymbol{k}_3}\,k_2^3\,\mathcal{P}_{_{\rm T}}(k_3)\right]\right\}^{-1}, \\
h_{\rm NL} &= -\left(\frac{4}{2\,\pi^2}\right)^2\,\left[k_1^3\,k_2^3\,k_3^3\,G_{\gamma\gamma\gamma}^{m_1 n_1 m_2 n_2 m_3 n_3}(\boldsymbol{k}_1,\boldsymbol{k}_2,\boldsymbol{k}_3)\right] \\
&\quad\times\left[\Pi_{m_1 n_1,m_2 n_2}^{\boldsymbol{k}_1}\,\Pi_{m_3 n_3,\bar{m}\bar{n}}^{\boldsymbol{k}_2}\,k_3^3\,\mathcal{P}_{_{\rm T}}(k_1)\,\mathcal{P}_{_{\rm T}}(k_2)+\text{five permutations}\right]^{-1}.
\end{aligned}
$$

[29] V. Sreenath, R. Tibrewala and L. Sriramkumar, JCAP **1312**, 037 (2013).

The actions governing the other three point functions

The actions that lead to the correlations involving two scalars and one tensor, one scalar and two tensors and three tensors are given by[30]

$$S^3_{\mathcal{R}\mathcal{R}\gamma}[\mathcal{R},\gamma_{ij}] = M_{_{\mathrm{Pl}}}^2 \int \mathrm{d}\eta \int \mathrm{d}^3\boldsymbol{x}\, \biggl[a^2\,\epsilon_1\,\gamma_{ij}\,\partial_i\mathcal{R}\,\partial_j\mathcal{R} + \frac{1}{4}\,\partial^2\gamma_{ij}\,\partial_i\chi\,\partial_j\chi + \frac{a\,\epsilon_1}{2}\,\gamma_{ij}'\,\partial_i\mathcal{R}\,\partial_j\chi + \mathcal{F}^2_{ij}(\mathcal{R})\,\frac{\delta\mathcal{L}^2_{\gamma\gamma}}{\delta\gamma_{ij}} + \mathcal{F}^3(\mathcal{R},\gamma_{ij})\,\frac{\delta\mathcal{L}^2_{\mathcal{R}\mathcal{R}}}{\delta\mathcal{R}}\biggr],$$

$$S^3_{\mathcal{R}\gamma\gamma}[\mathcal{R},\gamma_{ij}] = \frac{M_{_{\mathrm{Pl}}}^2}{4} \int \mathrm{d}\eta \int \mathrm{d}^3\boldsymbol{x}\, \biggl[\frac{a^2\,\epsilon_1}{2}\,\mathcal{R}\,\gamma_{ij}'\,\gamma_{ij}' + \frac{a^2\,\epsilon_1}{2}\,\mathcal{R}\,\partial_l\gamma_{ij}\,\partial_l\gamma_{ij} - a\,\gamma_{ij}'\,\partial_l\gamma_{ij}\,\partial_l\chi + \mathcal{F}^4_{ij}(\mathcal{R},\gamma_{mn})\,\frac{\delta\mathcal{L}^2_{\gamma\gamma}}{\delta\gamma_{ij}}\biggr],$$

$$S^3_{\gamma\gamma\gamma}[\gamma_{ij}] = \frac{M_{_{\mathrm{Pl}}}^2}{2} \int \mathrm{d}\eta \int \mathrm{d}^3\boldsymbol{x}\, \biggl[\frac{a^2}{2}\,\gamma_{lj}\,\gamma_{im}\,\partial_l\partial_m\gamma_{ij} - \frac{a^2}{4}\,\gamma_{ij}\,\gamma_{lm}\,\partial_l\partial_m\gamma_{ij}\biggr].$$

The quantities $\mathcal{L}^2_{\mathcal{R}\mathcal{R}}$ and $\mathcal{L}^2_{\gamma\gamma}$ are the second order Lagrangian densities comprising of two scalars and tensors which lead to the equations of motion.

[30] J. Maldacena, JHEP **0305**, 013 (2003).

Comparison between analytical and numerical results

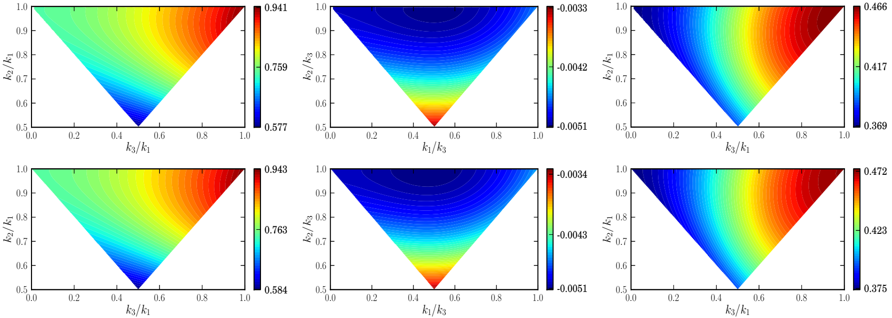

A comparison of the analytical results (at the bottom) for the non-Gaussianity parameters $C_{_{\rm NL}}^{\mathcal{R}}$ (on the left), $C_{_{\rm NL}}^{\gamma}$ (in the middle) and $h_{_{\rm NL}}$ (on the right) with the numerical results (on top) for a generic triangular configuration of the wavevectors in the case of the standard quadratic potential[31]. As in the case of the scalar bispectrum, the maximum difference between the numerical and the analytic results is about 5%.

[31] V. Sreenath, R. Tibrewala and L. Sriramkumar, JCAP **1312**, 037 (2013).

Three point functions for models with features

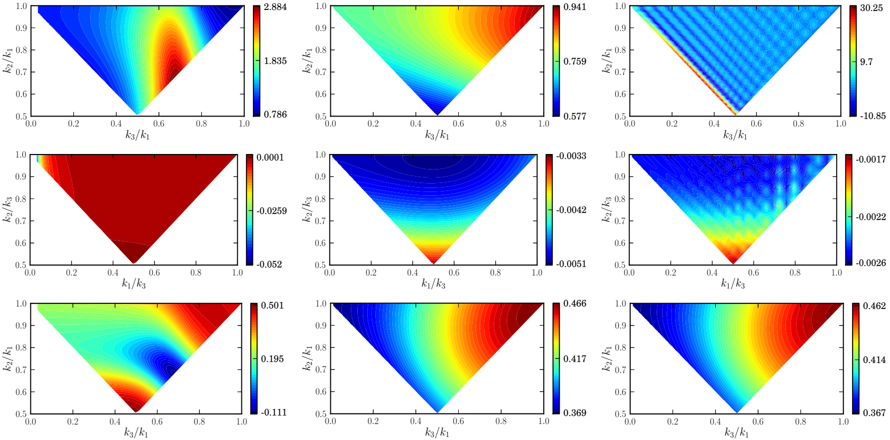

Density plots of the non-Gaussianity parameters $C_{\rm NL}^{\mathcal{R}}$ (on top), $C_{\rm NL}^{\gamma}$ (in the middle) and $h_{\rm NL}$ (at the bottom) evaluated numerically for an arbitrary triangular configuration of the wavevectors for the case of the punctuated inflationary scenario (on the left), the quadratic potential with the step (in the middle) and the axion monodromy model (on the right).

The effect of the long wavelength modes

Since the amplitude of a scalar or a tensor mode is a constant when they are well outside the Hubble radius, a long wavelength perturbation can be treated as a background as far as the smaller wavelength modes are concerned.

Let us denote the constant amplitude (*i.e.* as far as their time dependence is concerned) of the long wavelength scalar and tensor modes as, say, $\mathcal{R}^{\mathrm{B}}$ and γ_{ij}^{B}, respectively.

In the presence of such modes, the *background* FLRW metric will take the form

$$\mathrm{d}s^2 = -\mathrm{d}t^2 + a^2(t)\,\mathrm{e}^{2\,\mathcal{R}^{\mathrm{B}}}\,[\mathrm{e}^{\gamma^{\mathrm{B}}}]_{ij}\,\mathrm{d}\boldsymbol{x}^i\,\mathrm{d}\boldsymbol{x}^j,$$

i.e. the long wavelength modes lead to modified spatial coordinates.

Such a modification is completely equivalent to a spatial transformation of the form $\boldsymbol{x}' = \Lambda\,\boldsymbol{x}$, with the components of the matrix Λ being given by

$$\Lambda_{ij} = \mathrm{e}^{\mathcal{R}^{\mathrm{B}}}\,\left[\mathrm{e}^{\gamma^{\mathrm{B}}/2}\right]_{ij}.$$

The behavior of the two-point functions

One finds that the scalar and the tensor two-point functions in the presence of a long wavelength mode denoted by, say, the wavenumber k, can be written as

$$\begin{aligned}
\langle \hat{\mathcal{R}}_{\boldsymbol{k}_1}\, \hat{\mathcal{R}}_{\boldsymbol{k}_2} \rangle_k &= \frac{(2\,\pi)^2}{2\,k_1^3}\, \mathcal{P}_{_{\rm S}}(k_1)\, \delta^{(3)}(\boldsymbol{k}_1 + \boldsymbol{k}_2) \\
&\quad \times \left[1 - (n_{_{\rm S}} - 1)\, \mathcal{R}^{\rm B} - \left(\frac{n_{_{\rm S}} - 4}{2}\right) \gamma_{ij}^{\rm B}\, \hat{n}_{1i}\, \hat{n}_{1j}\right], \\
\langle \hat{\gamma}_{m_1 n_1}^{\boldsymbol{k}_1}\, \hat{\gamma}_{m_2 n_2}^{\boldsymbol{k}_2} \rangle_k &= \frac{(2\,\pi)^2}{2\,k_1^3}\, \frac{\Pi_{m_1 n_1, m_2 n_2}^{\boldsymbol{k}_1}}{4}\, \mathcal{P}_{_{\rm T}}(k_1)\, \delta^{(3)}(\boldsymbol{k}_1 + \boldsymbol{k}_2) \\
&\quad \times \left[1 - n_{_{\rm T}}\, \mathcal{R}^{\rm B} - \left(\frac{n_{_{\rm T}} - 3}{2}\right) \gamma_{ij}^{\rm B}\, \hat{n}_{1i}\, \hat{n}_{1j}\right],
\end{aligned}$$

where $\hat{n}_{1i} = k_{1i}/k_1$.

The behavior of the three-point functions

One can also show that, in the presence of a long wavelength mode, the three-point functions can be written as

$$
\begin{aligned}
\langle \hat{\mathcal{R}}_{\boldsymbol{k}_1} \hat{\mathcal{R}}_{\boldsymbol{k}_2} \hat{\mathcal{R}}_{\boldsymbol{k}_3} \rangle_{k_3} &\equiv \langle \langle \hat{\mathcal{R}}_{\boldsymbol{k}_1} \hat{\mathcal{R}}_{\boldsymbol{k}_2} \rangle_{k_3} \hat{\mathcal{R}}_{\boldsymbol{k}_3} \rangle \\
&= -\frac{(2\,\pi)^{5/2}}{4\,k_1^3\,k_3^3}\,(n_{\mathrm{S}}-1)\,\mathcal{P}_{\mathrm{S}}(k_1)\,\mathcal{P}_{\mathrm{S}}(k_3)\,\delta^3(\boldsymbol{k}_1+\boldsymbol{k}_2),\\
\langle \hat{\mathcal{R}}_{\boldsymbol{k}_1} \hat{\mathcal{R}}_{\boldsymbol{k}_2} \hat{\gamma}^{\boldsymbol{k}_3}_{m_3 n_3} \rangle_{k_3} &\equiv \langle \langle \hat{\mathcal{R}}_{\boldsymbol{k}_1} \hat{\mathcal{R}}_{\boldsymbol{k}_2} \rangle_{k_3} \hat{\gamma}^{\boldsymbol{k}_3}_{m_3 n_3} \rangle \\
&= -\frac{(2\,\pi)^{5/2}}{4\,k_1^3\,k_3^3}\left(\frac{n_{\mathrm{S}}-4}{8}\right)\mathcal{P}_{\mathrm{S}}(k_1)\,\mathcal{P}_{\mathrm{T}}(k_3)\\
&\quad\times \Pi^{\boldsymbol{k}_3}_{m_3 n_3,ij}\,\hat{n}_{1i}\,\hat{n}_{1j}\,\delta^3(\boldsymbol{k}_1+\boldsymbol{k}_2),\\
\langle \hat{\mathcal{R}}_{\boldsymbol{k}_1} \hat{\gamma}^{\boldsymbol{k}_2}_{m_2 n_2} \hat{\gamma}^{\boldsymbol{k}_3}_{m_3 n_3} \rangle_{k_1} &\equiv \langle \hat{\mathcal{R}}_{\boldsymbol{k}_1} \langle \hat{\gamma}^{\boldsymbol{k}_2}_{m_2 n_2} \hat{\gamma}^{\boldsymbol{k}_3}_{m_3 n_3} \rangle_{k_1} \rangle \\
&= -\frac{(2\,\pi)^{5/2}}{4\,k_1^3\,k_2^3}\,\frac{n_{\mathrm{T}}}{4}\,\mathcal{P}_{\mathrm{S}}(k_1)\,\mathcal{P}_{\mathrm{T}}(k_2)\,\Pi^{\boldsymbol{k}_2}_{m_2 n_2,m_3 n_3}\,\delta^3(\boldsymbol{k}_2+\boldsymbol{k}_3),\\
\langle \hat{\gamma}^{\boldsymbol{k}_1}_{m_1 n_1} \hat{\gamma}^{\boldsymbol{k}_2}_{m_2 n_2} \hat{\gamma}^{\boldsymbol{k}_3}_{m_3 n_3} \rangle_{k_3} &\equiv \langle \langle \hat{\gamma}^{\boldsymbol{k}_1}_{m_1 n_1} \hat{\gamma}^{\boldsymbol{k}_2}_{m_2 n_2} \rangle_{k_3} \hat{\gamma}^{\boldsymbol{k}_3}_{m_3 n_3} \rangle \\
&= -\frac{(2\,\pi)^{5/2}}{4\,k_1^3\,k_3^3}\left(\frac{n_{\mathrm{T}}-3}{32}\right)\mathcal{P}_{\mathrm{T}}(k_1)\,\mathcal{P}_{\mathrm{T}}(k_3)\\
&\quad\times \Pi^{\boldsymbol{k}_1}_{m_1 n_1,m_2 n_2}\,\Pi^{\boldsymbol{k}_3}_{m_3 n_3,ij}\,\hat{n}_{1i}\,\hat{n}_{1j}\,\delta^3(\boldsymbol{k}_1+\boldsymbol{k}_2).
\end{aligned}
$$

Consistency relations in the squeezed limit

Upon making use of the above expressions for the three-point functions in the definitions for the non-Gaussianity parameters, we can express the consistency relations in the squeezed limit as follows[32]:

$$
\begin{aligned}
\lim_{k_3\to 0} f_{\rm NL}(\boldsymbol{k},-\boldsymbol{k},\boldsymbol{k}_3) &= \frac{5}{12}\,\left[n_{\rm S}(k)-1\right],\\
\lim_{k_3\to 0} C_{\rm NL}^{\mathcal{R}}(\boldsymbol{k},-\boldsymbol{k},\boldsymbol{k}_3) &= \left[\frac{n_{\rm S}(k)-4}{4}\right]\,\left(\Pi^{\boldsymbol{k}_3}_{m_3n_3,\bar{m}\bar{n}}\right)^{-1}\,\Pi^{\boldsymbol{k}_3}_{m_3n_3,ij}\,\hat{n}_i\,\hat{n}_j,\\
\lim_{k_1\to 0} C_{\rm NL}^{\gamma}(\boldsymbol{k}_1,\boldsymbol{k},-\boldsymbol{k}) &= \frac{n_{\rm T}(k)}{2}\,\left(\Pi^{\boldsymbol{k}}_{m_2n_2,m_3n_3}\right)^{-1}\,\Pi^{\boldsymbol{k}}_{m_2n_2,m_3n_3},\\
\lim_{k_3\to 0} h_{\rm NL}(\boldsymbol{k},-\boldsymbol{k},\boldsymbol{k}_3) &= \left[\frac{n_{\rm T}(k)-3}{2}\right]\,\Bigl(2\,\Pi^{\boldsymbol{k}}_{m_1n_1,m_2n_2}\,\Pi^{\boldsymbol{k}_3}_{m_3n_3,\bar{m}\bar{n}}\\
&\quad +\Pi^{\boldsymbol{k}}_{m_1n_1,\bar{m}\bar{n}}\,\Pi^{\boldsymbol{k}_3}_{m_3n_3,m_2n_2}+\Pi^{\boldsymbol{k}}_{\bar{m}\bar{n},m_2n_2}\,\Pi^{\boldsymbol{k}_3}_{m_3n_3,m_1n_1}\Bigr)^{-1}\\
&\quad \times\Pi^{\boldsymbol{k}}_{m_1n_1,m_2n_2}\,\Pi^{\boldsymbol{k}_3}_{m_3n_3,ij}\,\hat{n}_i\,\hat{n}_j.
\end{aligned}
$$

[32] J. Maldacena, JHEP **0305**, 013 (2003);
P. Creminelli and M. Zaldarriaga, JCAP **0410**, 006 (2004);
D. Jeong and M. Kamionkowski, Phys. Rev. Lett. **108**, 251301 (2012);
S. Kundu, JCAP **1404**, 016 (2014);
V. Sreenath and L. Sriramkumar, JCAP **1410**, 021 (2014).

Consistency relations away from slow roll I

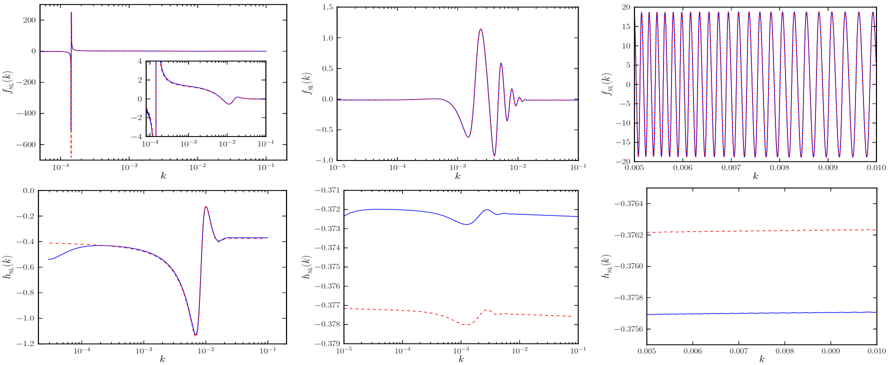

The behavior of the quantities $f_{\rm NL}$ (on top) and $h_{\rm NL}$ (at the bottom) in the squeezed limit has been plotted as a function of the wavenumber in the case of the punctuated inflationary scenario (on the left), the quadratic potential with a step (in the middle) and the axion monodromy model (on the right). The solid blue curves represent the numerical results obtained from the three-point functions, while the red dashed curves denote those arrived at using the consistency relations[33].

[33] V. Sreenath, D. K. Hazra and L. Sriramkumar, arXiv:1410.0252 [astro-ph.CO]; V. Sreenath and L. Sriramkumar, JCAP 1410, 021 (2014).

Consistency relations away from slow roll II

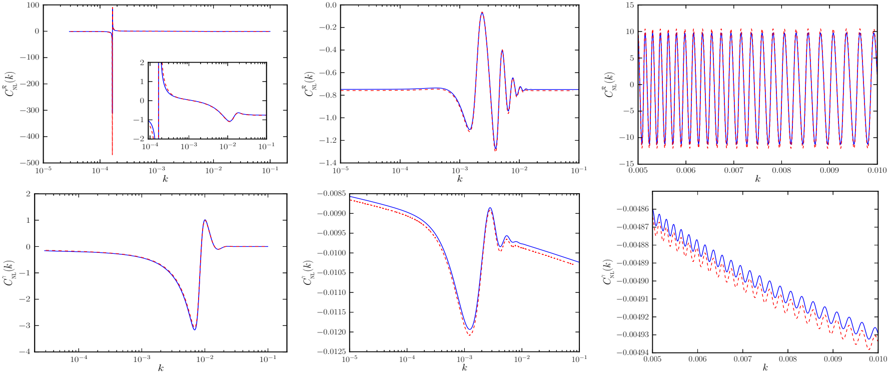

The behavior of the quantities $C_{\rm NL}^{\mathcal{R}}$ (on top) and $C_{\rm NL}^{\gamma}$ (at the bottom) in the squeezed limit has been plotted as a function of the wavenumber for the three models of interest as in the previous figure. Evidently, the good match between the solid blue curves and the red dashed ones indicate the validity of the consistency relations even in situations involving strong departures from slow roll as in punctuated inflation.

Summary

- The strong constraints on the non-Gaussianity parameter $f_{\rm NL}$ from Planck suggests that inflationary and post-inflationary scenarios that lead to rather large non-Gaussianities are very likely to be ruled out by the data.
- In contrast, various analyses seem to point to the fact that the scalar power spectrum may contain features[34]. The possibility of such features can provide a strong handle on constraining inflationary models. Else, one may need to carry out a systematic search involving the scalar and the tensor power spectra[35], the scalar and the tensor bispectra and the cross correlations to arrive at a small subset of viable inflationary models[36].
- Interestingly, we find that, in single field inflationary models, the consistency conditions governing the three-point functions remain valid even in situations involving sharp departures from slow roll. Observational evidence of deviations from the consistency conditions can provide a powerful constraint, possibly ruling out all single field inflationary models.

[34] P. A. R. Ade *et al.*, arXiv:1303.5082 [astro-ph.CO].

[35] In this context, see J. Martin, C. Ringeval and V. Vennin, arXiv:1303.3787 [astro-ph.CO].

[36] J. R. Fergusson, H. F. Gruetjen, E. P. S. Shellard and M. Liguori, arXiv:1410.5114 [astro-ph.CO].

Thank you for your attention